Supporting Information for:

Single-Molecule Folding of U2/U6 snRNAs Reveals Structural Dynamics Important for Splicing

Zhuojun Guo, Krishanthi S. Karunatilaka and David Rueda*

Department of Chemistry, Wayne State University, Detroit MI 48202

Corresponding author:

email: rueda@chem.wayne.edu, phone: (313) 577-6918, fax: (313) 577-8822

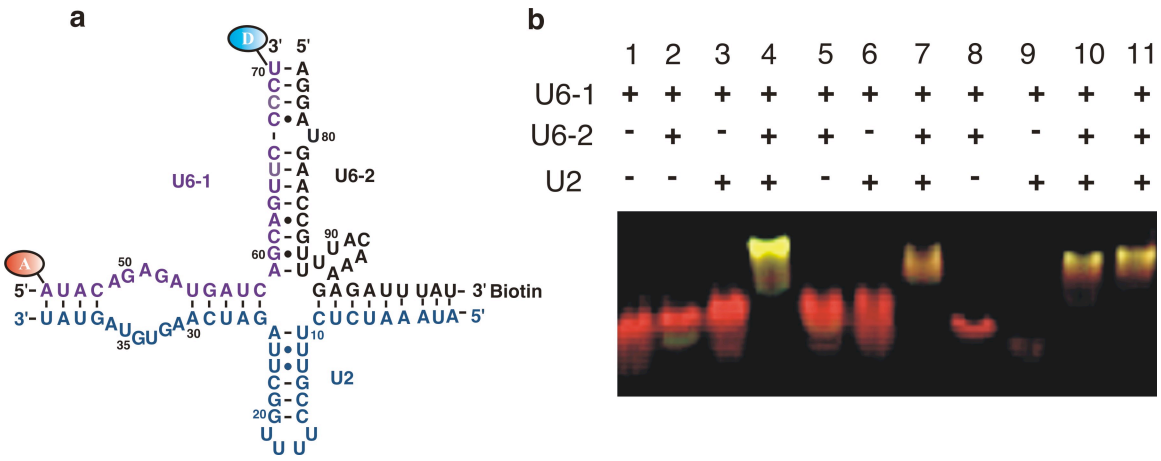

Supplementary Figure 1. (a) Labeled U2/U6 construct. This complex consists of 3 strands, U6-1 (purple), U6-2 (black) and U2 (blue). The 5' end of U6-1 is labeled with a FRET acceptor (Cy5) and the 3' end is labeled with a FRET donor (Cy3). The 3' end of U6-2 is conjugated to biotin for surface immobilization. (b) Formation of the fluorophore-labeled U2/U6 complex monitored by non-denaturing gel electrophoresis with fluorescence detection. Each sample was prepared as in the FRET experiments. This 15% (wt/vol) polyacrylamide gel was run at 4 °C (20 mM Tris-Acetic acid, pH 7.5, 20 mM NaOAc, 40 mM $Mg(OAc)_2$) and 6 volts/cm. **Lane 1**: 10 pmol of fluorophore labeled U6-1 only. The red (high FRET) RNA migrates as a single band indicating its purity. **Lane 2**: 10 pmol of fluorophore labeled U6-1 and 20 pmol of biotinylated U6-2. The red (high FRET) RNA migrates as a single band indicating that these two RNAs alone do not from a stable U6-1/U6-2 complex. **Lane 3**: 10 pmol of fluorophore labeled U6-1 and 40 pmol of U2. The band migrates as in lane 1 indicating that these two RNAs alone do not from a stable U6-1/U2 complex. **Lane 4**: 10 pmol of fluorophore labeled U6-1, 20 pmol of biotinylated U6-2 and 40 pmol of U2. A yellow (low-mid FRET) slow migrating band clearly shows the formation of the ternary U6-1/U6-2/U2 complex. **Lane 5**: 10 pmol of fluorophore labeled triad mutant U6-1 and 20 pmol of biotinylated triad mutant U6-2. The red (high FRET) RNA migrates

as a single band indicating that these two RNAs alone do not from a stable U6-1/U6-2 complex. **Lane 6**: 10 pmol of fluorophore labeled triad U6-1 and 40 pmol of U2. The band migrates as in lane 1 indicating that these two RNAs alone do not from a stable U6-1/U2 complex. **Lane 7**: 10 pmol of fluorophore labeled triad mutant U6-1, 20 pmol of biotinylated triad mutant U6-2 and 40 pmol of U2. An orange (mid FRET) slow migrating band clearly shows the formation of the ternary triad mutant U6-1/U6-2/U2 complex. **Lane 8**: 10 pmol of fluorophore labeled single mutant U6-1 and 20 pmol of biotinylated U6-2. The red (high FRET) RNA migrates as a single band indicating that these two RNAs alone do not from a stable U6-1/U6-2 complex. **Lane 9**: 10 pmol of fluorophore labeled single mutant U6-1 and 40 pmol of U2. The band migrates as in lane 1 indicating that these two RNAs alone do not from a stable U6-1/U2 complex. **Lane 10**: 10 pmol of fluorophore labeled single mutant U6-1, 20 pmol of biotinylated U6-2 and 40 pmol of U2. A yellow-orange (low-mid FRET) slow migrating band clearly shows the formation of the ternary single mutant U6-1/U6-2/U2 complex. **Lane 11**: 10 pmol of fluorophore labeled single mutant U6-1, 20 pmol of biotinylated U6-2 and 40 pmol of double mutant U2. A yellow-orange (low-mid FRET) slow migrating band clearly shows the formation of the ternary double mutant U6-1/U6-2/U2 complex.

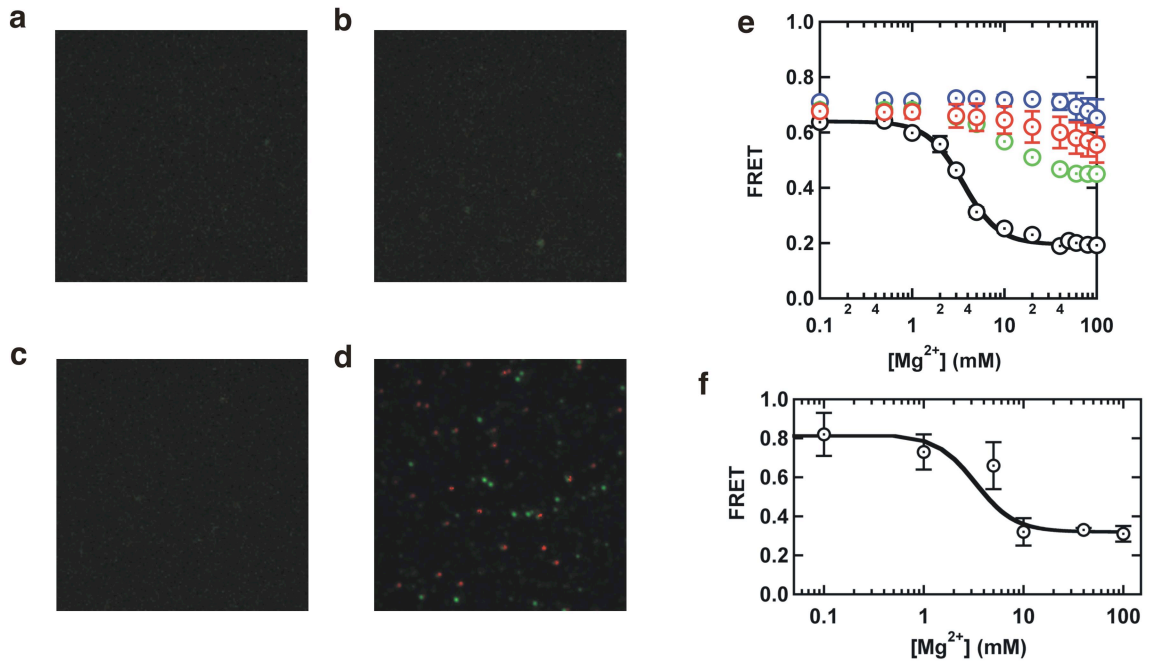

Supplementary Figure 2. (a, b, c, d) smFRET control experiments testing how the heterogeneity affects the single molecule measurements. (a) Slide with only Cy3 and Cy5 labeled U6-1. Without biotin, U6-1 alone cannot be immobilized on the slide surface, and no molecules are observed. (b) Slide with U6-1 and U6-2. There are only very few molecules on the slide because the U6-1/U6-2 complex alone is not stable, consistent with the non-denaturing gel electrophoresis (see Supplementary Figure 1b). The surface density of immobilized molecules is 20-fold lower than that of the 3-strand complex. (c) Slide with U6-1 and U2. No molecule is immobilized on the slide surface because there is no biotin present. (d) Slide with U6-1, U6-2 and U2. The 3-strand complex can form stably (see Supplementary Figure 1b), and it can be immobilized on the slide surface efficiently. The buffer conditions for all these experiments are 50 mM Tris-HCl, pH 7.5, 10 mM $MgCl_2$, 100 mM NaCl. (e) Ensemble-averaged magnesium titration of the fluorophore labeled three-strand complex (black), U6-1 alone (blue), U6-1/U2 (red), and U6-1/U6-2 (green). Only the three-strand complex exhibits a significant Mg^{2+}

dependent conformational change. These data, together with Supplementary Figure 2a, b, c, d show that the observed conformational dynamics reflect only the behavior of the three-strand complex. The buffer condition for this experiment is 50 mM Tris-HCl, pH 7.5, 100 mM NaCl and 25 mM DTT. (f) Comparison of the Mg^{2+} titration in ensemble-averaged and single-molecule experiments. The calculated average FRET values from the single-molecule histograms in Figure 2d (circles) overlay within error on the fit of the ensemble averaged measurements from Figure 1e (line). The error bars stem from the standard deviation of the single-molecule FRET distributions. The initial and final FRET values of the fit had to be adjusted because the filters used in the two experiments are different yielding somewhat different initial and final FRET values, but the K_{Mg} and the Hill coefficient n were held constant to their values in Figure 1e. This results shows that the surface immobilization scheme does not significantly affect the U2/U6 structural dynamics. The buffer conditions for these smFRET experiments are 50 mM Tris-HCl, pH 7.5, 100 mM NaCl, and for bulk titration 50 mM Tris-HCl, pH 7.5, 100mM NaCl and 25mM DTT.

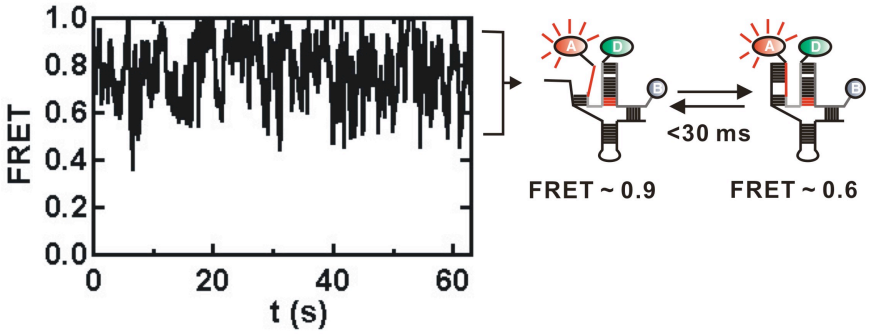

Supplementary Figure 3. Single-molecule time trajectory in the absence of Mg^{2+}. The trace is smoothed with a running 5-point average. The FRET value oscillates randomly between 1.0 and 0.5 without the presence of well-defined conformational states. The observed oscillations are much wider than our experimental noise indicating the presence of dynamics faster than our 33 ms time resolution. These dynamics result in the broad distributions in Figure 2d. A possible explanation is that the 5'end of U6 does not base pair stably with U2 in the absence of Mg^{2+}. The buffer condition for this experiment is 50 mM Tris-HCl, pH 7.5, 0 mM $MgCl_2$, 100 mM NaCl.

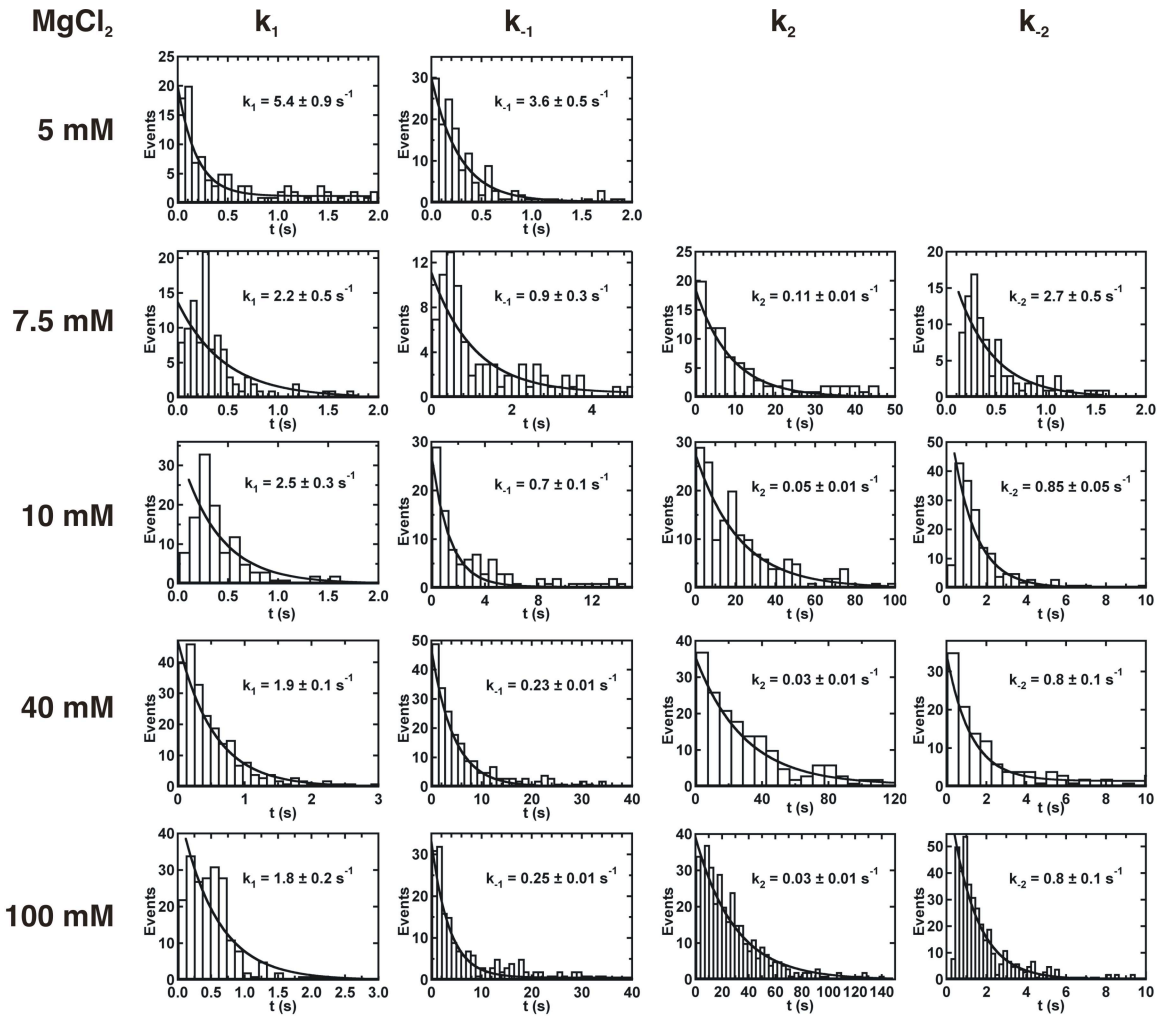

Supplementary Figure 4. Dwell time analysis for the rate constants k_1 (column1), k_{-1} (column2), k_2 (column3) and k_{-2} (column4) as a function of [Mg^{2+}]. The pseudo-first order rates were determined by fitting the dwell time distributions to single exponential decays (black lines). The resulting values were used in Fig 3b. The buffer conditions for these experiments are 50 mM Tris-HCl, pH 7.5, 100 mM NaCl and variable [Mg^{2+}].

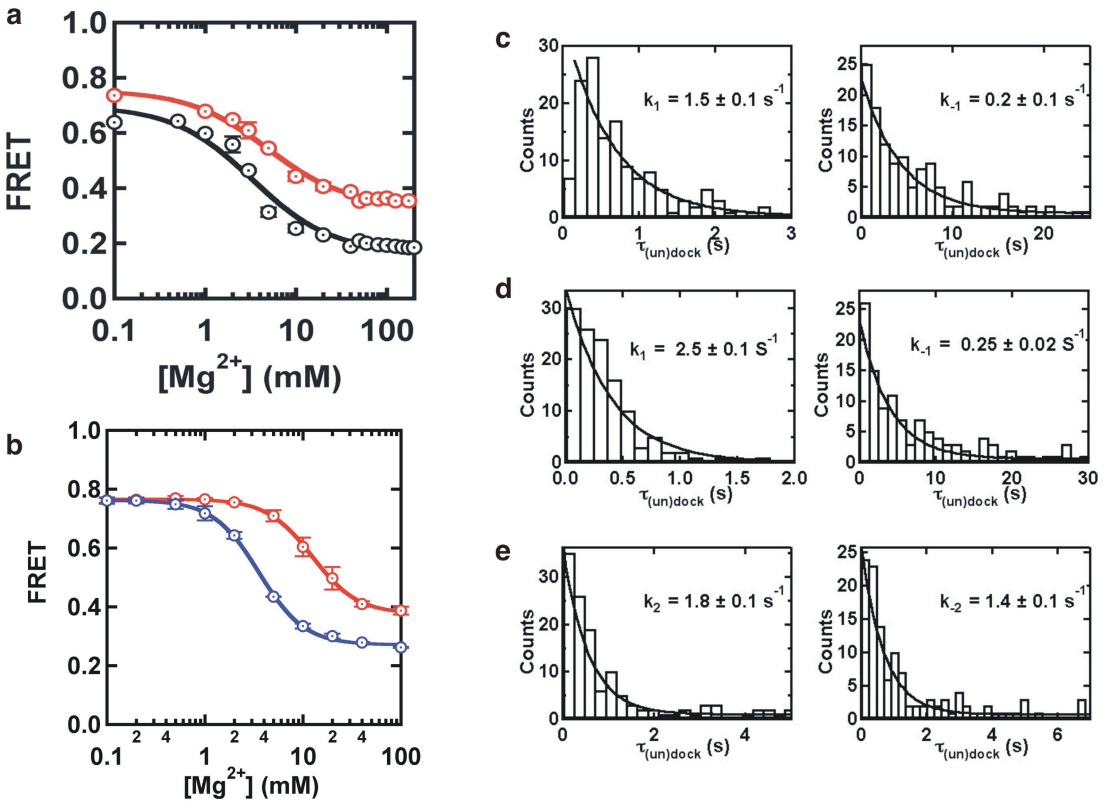

Supplementary Figure 5. (a) Ensemble-averaged magnesium titration of the fluorophore labeled U2/U6 complex with the six fold flipped-triad mutations (red). A fit to the modified Hill equation yields a dissociation constant K_{Mg} = 4.8 ± 0.5 mM, similar to the wild type (black). However, the observed FRET ratio at high [Mg^{2+}] is significantly higher than the wild type (black), in agreement with the single-molecule data for this mutant (Figure 4a). This data supports that Helix IB only forms in the low FRET state (G). The buffer condition for this experiment is 50 mM Tris-HCl, pH 7.5, 100mM NaCl and 25mM DTT. (b) Ensemble-averaged magnesium titration of the fluorophore labeled U2/U6 complex with an A59C mutation in U6 (red). A fit to the modified Hill equation yields a dissociation constant K_{Mg} = 12.4 ± 0.4 mM (red line), four-fold larger than the wild-type. In addition, the observed FRET ratio at high [Mg^{2+}] is significantly higher than the wild type (Supplementary Figure 5a, black), in agreement with the

single-molecule data for this mutant (Figure 4c). Magnesium titration with the compensatory mutation in U23G in U2 (blue). A fit to the modified Hill equation yields a dissociation constant K_{Mg} = 3.6 ± 0.1 mM for the double mutant (blue line), in excellent agreement with the wild type and the single-molecule experiments for this mutant (Figure 4d). The buffer condition for this experiment is 50 mM Tris-HCl, pH 7.5, 100 mM NaCl and 25 mM DTT. (c, d, e) Dwell time analysis for the rate constants of triad mutant, single mutant and A91G mutant. (c) Dwell time analysis for the rate constants k_1, k_{-1} of triad mutant. The values are comparable to that of the wild-type U2/U6 complex (Supplementary Figure 4), suggesting that the six-fold mutation does not affect the transition between N and I. (d) Dwell time analysis for the rate constants k_1, k_{-1} of A59C single mutant. The values are comparable to that of the wild-type U2/U6 complex (Supplementary Figure 4), suggesting that A59C mutation does not affect the transition between the N and I. (e) Dwell time analysis for the rate constants k_2, k_{-2} of A91G mutant. The value of k_{-2} is comparable to that of wild type, while the k_2 is 60-fold larger than that of wild type (Supplementary Figure 4). This indicates that this mutation favors the formation of G. The buffer conditions for these experiments are 50 mM Tris-HCl, pH 7.5, 40 mM $MgCl_2$, 100 mM NaCl.

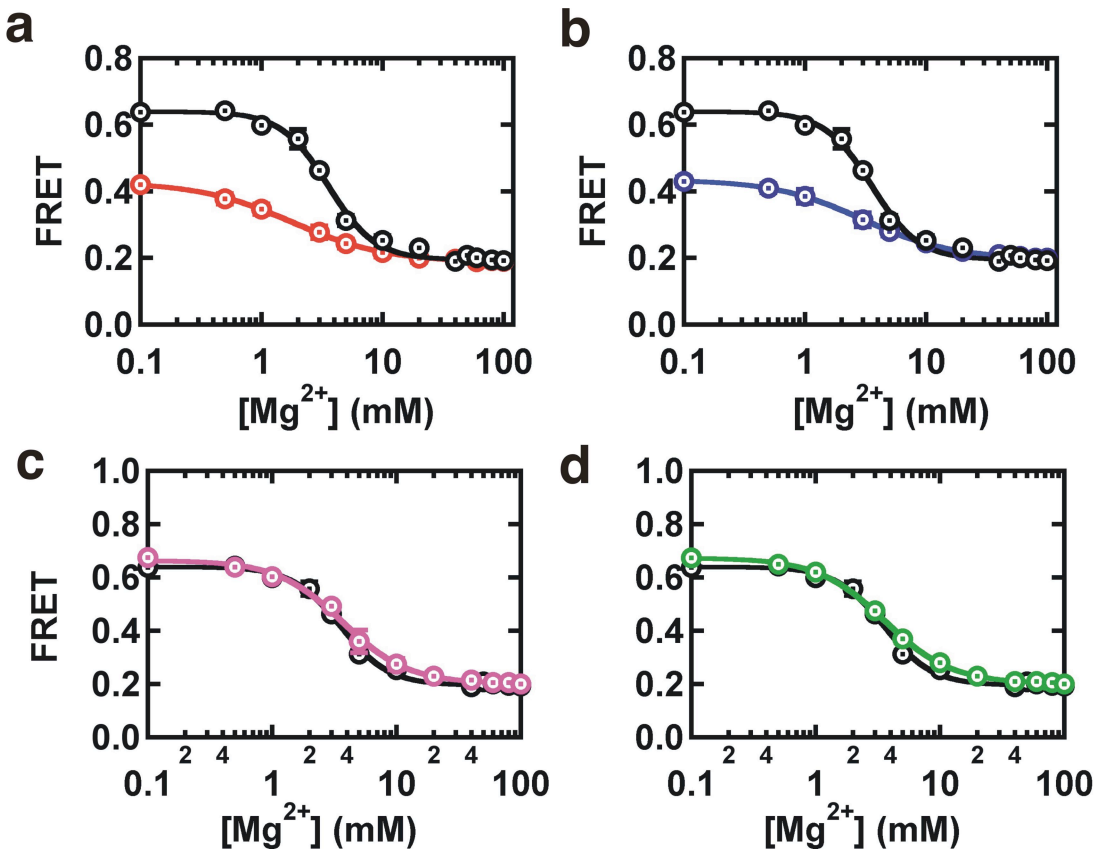

Supplementary Figure 6. Ensemble-averaged magnesium titration of the fluorophore labeled U2/U6 complex with U80 deletion (red), U80G (Blue), U80A (pink) and U80C (green) mutations compared with the WT (black). A fit to the modified Hill equation yields dissociation constants for these U80 mutants K_{Mg} = 1.8 ± 0.1 mM, 3.0 ± 0.1 mM, 3.6 ± 0.1 mM and 3.6 ± 0.2 mM, respectively, and cooperativity coefficients n = 1.1 ± 0.1, 1.1 ± 0.1, 1.6 ± 0.1 and 1.6 ± 0.1, respectively. With U80 deletion and U80G mutant, the observed FRET ratio at Low [Mg^{2+}] is significantly lower than the wild type (black), in agreement with the disappearance of the high FRET conformation observed in the single-molecule data for this mutant (Figure 5). However, the data for the U80A and U80C mutants overlaps with that of the WT. This data suggests that U80 plays an important role in stabilizing the high FRET conformation. The buffer condition for this experiment is 50 mM Tris-HCl, pH 7.5, 100 mM NaCl and 25 mM DTT.

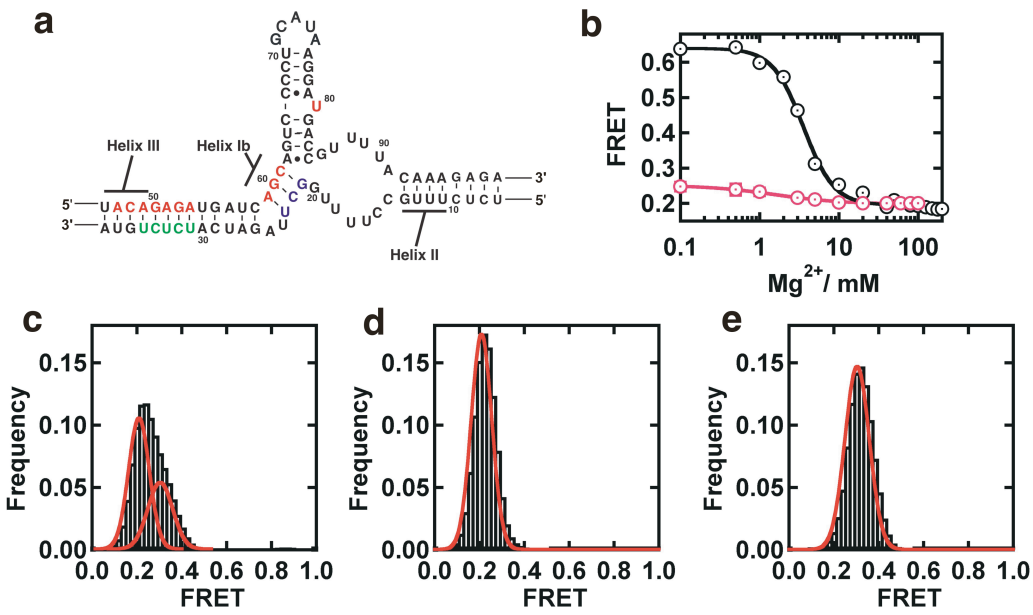

Supplementary Figure 7. Ensemble-averaged magnesium titration and single molecule data for the ACAGAGA loop deletion mutant. (a) The construct with ACAGAGA loop deletion used. The U2 bases in green were mutated to base pair with the ACAGAGA sequence in U6. (b) Ensemble-averaged magnesium titration of this construct and the observed FRET ratio of ACAGAGA loop deletion (red) at Low [Mg^{2+}] is significantly lower than the wild type (black). The buffer conditions for this experiment are 50 mM Tris-HCl, pH 7.5, 100 mM NaCl and 25 mM DTT (c) The smFRET histogram of ACAGAGA loop deletion mutant in 5 mM $MgCl_2$. There are 2 major peaks at ~0.2 and ~0.3 FRET, and (d) The smFRET histogram of 0.2 state population in 5 mM $MgCl_2$. The percentage of molecules in 0.2 state to all the single molecules is 28.4%. (e) The smFRET histogram of 0.3 state population in 5mM $MgCl_2$. The percentage of molecules in 0.3 state to all the single molecules is 66.7%. The buffer conditions for these experiments are 50 mM Tris-HCl, pH 7.5, 5 mM $MgCl_2$, 100 mM NaCl.

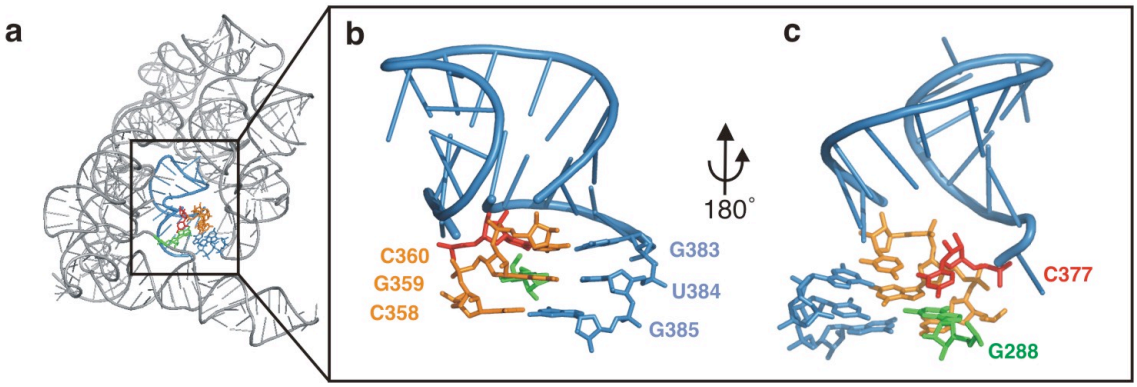

Supplementary Figure 8. The recent crystal structure of the self-splicing Group II intron ribozyme supports the hypothesis that the high FRET conformation resembles the active conformation adopted during splicing given the similarity between the U6 ISL and the domain 5 of Group II intron. (a) The crystal structure of the whole self-splicing Group II intron. The boxed region is the catalytic active domain 5. (b) and (c) Higher magnifications of the boxed region (domain 5). In this structure, $C_{358}G_{359}C_{360}$ (equivalents of the AGC triad, orange) are clearly base paired with $G_{383}U_{384}G_{385}$ (blue), extending domain 5 (equivalent of the U6 ISL). In addition, the C360-G383 base pair forms a base triple with C377 (equivalent of U80, red), which in turn forms a base stacking interaction with G288 from J2/3 (equivalent of the ACAGAGA loop, green). Finally, G288 forms a base triple with the G359-U384 base pair as well. All these interactions could readily take place in the high FRET structure observed in this paper. [Structure according to Toor, N. *et al.* (2008) Science **320**:77].

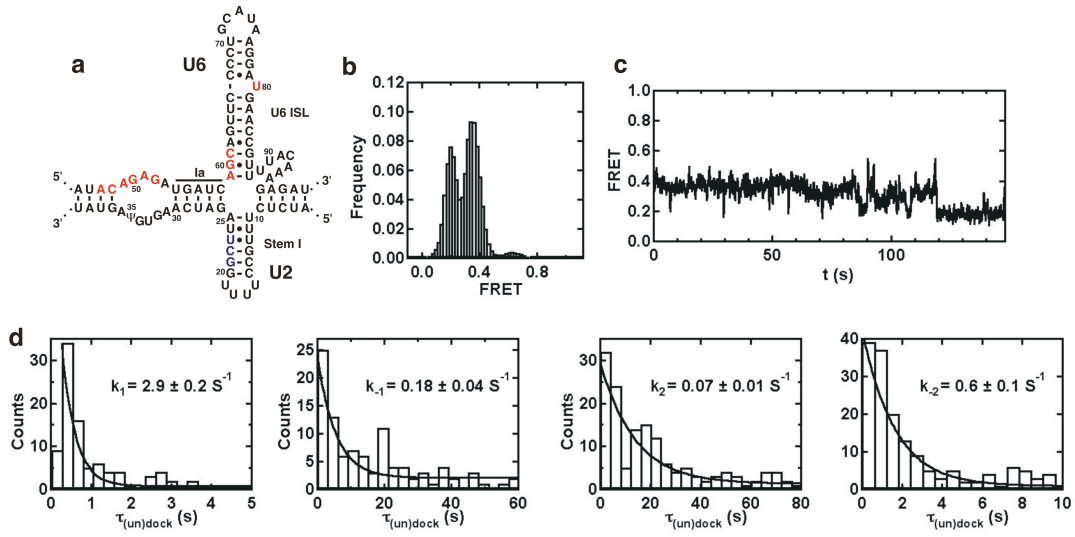

Supplementary Figure 9. Single molecule data for the construct with an intact GNRUA loop. (A) The construct with GNRUA loop used in smFRET experiments. The donor fluorophore is at the 5' end of U6, the acceptor is on the U6 base U70 and the biotin is on the 3' end of U6, equivalent to the three strand construct (Supplementary Figure 1a). (B) FRET histogram of this 2-strand construct in 40 mM $MgCl_2$ There are 2 major peaks at FRET 0.2 and 0.4, which are comparable to that of the 3-strand construct (Figure 2d). (C) Single-molecule trajectory of the 2-strand construct. The molecule shows dynamic transitions between the 0.2, 0.4 and 0.6 states, which are similar to the wild type (Figure 2b). (D) Dwell time analysis for the rate constants of the 2-strand construct. The resulting folding rate constants for the two-strand construct are all within two-fold of the three-strand construct folding rates (Supplementary Figure 4). These smFRET data of the 2-strand U2/U6 complex validate the use of the three-strand construct. The buffer conditions for these experiments are 50 mM Tris-HCl, pH 7.5, 40 mM $MgCl_2$, 100 mM NaCl.